Article:
Wang, H, Lin, G, Shen, X et al. (2019) Effect of evaporator tilt on a loop heat pipe with non-condensable gas. International Journal of Heat and Mass Transfer, 128. pp. 1072-1080. ISSN: 0017-9310

https://doi.org/10.1016/j.ijheatmasstransfer.2018.09.033

Effect of evaporator tilt on a loop heat pipe with non-condensable gas

Huanfa Wang[1], Guiping Lin[1], Xiaobin Shen[1,2,*], Lizhan Bai[1], Dongsheng Wen[1,2]

1 Laboratory of Fundamental Science on Ergonomics and Environmental Control, School of Aeronautic Science and Engineering, Beihang University, Beijing 100191, China

2 School of Chemical and Processing Engineering, University of Leeds, Leeds, LS2 9JT, UK

Abstract: The coupling effect of non-condensable gas (NCG) and evaporator tilts on the steady state operation of a loop heat pipe (LHP) was investigated both experimentally and theoretically in this work. Nitrogen was injected quantitatively into an ammonia-stainless steel LHP to simulate NCG, and the steady state characteristics of the LHP were studied under three typical evaporator tilts. According to the experimental results, the main conclusions below can be drawn. (1) The temperature is the highest under adverse tilt and the lowest under favorable tilt no matter whether there is NCG in LHP. (2) The existence of NCG could cause the increase of temperature under all three typical evaporator tilts, but the temperature increment caused by NCG seems to be relatively small under adverse tilt. (3) The increments of the temperature caused by NCG display different patterns under different tilts. Theoretical analysis was conducted to explain the results: the temperature under the coupling effect of NCG and evaporator tilt was determined by the energy balance between the heat leak from evaporator to compensation chamber and the cooling capacity of returning subcooled liquid. With the increase of heat load, the augmentation of heat leak caused by NCG and the enhancement of subcooled liquid cooling effect were incongruent. The coupling effect of NCG and evaporator tilts should be considered in the terrestrial application of LHP.

Keywords: Loop heat pipe; Non-condensable gas; Evaporator tilt; Steady state operation; Energy balance

1. Introduction

Loop heat pipe (LHP) is an efficient and reliable two-phase heat-transfer device that utilizes the phase change of working fluid between heat source and heat sink to transfer heat. The capillary force developed in the efficient porous structure is the driving force that circulates the working fluid in the loop[1,2]. Compared with traditional heat pipe, LHP possesses many unique advantages such as high heat transfer capacity and flexible application[3–5], and has been applied to aerospace field for many years[6–8].

However, degradation of LHP performance has been found in practical spacecraft application[9–11]. The non-condensable gas (NCG) produced during the operation of LHP was believed to be responsible for the performance degradation and lifespan issues of LHP[12]. NCG is the gas that cannot condense into liquid phase within the operating temperature range of the two-phase systems. In recent years, a few studies about the NCG effect on the performance of LHP have been conducted, and corresponding solutions have been studied as well. Ref [13] and Ref [14] studied the impacts of NCG on the steady state characteristics of LHP by injecting NCG into LHP quantificationally. Experiments showed that the operation of LHP was insensitive to the presence of NCG compared with conventional heat pipes, but NCG would increase the startup time and operating temperature. Ref [15] investigated the heat transport characteristics of reservoir embedded loop heat pipe with different NCG inventories by experiment and calculation. It was found that NCG increased the operating temperature due to the partial pressure of NCG in compensation chamber (CC) and the effect was more significant when the heat load was small. Ref [16] investigated the effects of NCG on the operating characteristics of LHP systemically, including temperature hysteresis phenomenon. Besides, in the operating of LHP with NCG, distinct temperature oscillation phenomenon was observed. Ref [17] designed a LHP that can operate at 125 °C, and tested the operating performance in the case with NCG. Ref [18] investigated the control effect of thermoelectric cooler on the

operating of LHP and found that the application of thermoelectric cooler could significantly reduce the temperature rise caused by NCG.

Recently, LHP technology has been developed for aircraft applications and the gas/liquid distribution in LHP would be affected significantly by gravity, which is quite different from the case in space [19,20]. It seems that the relative position between evaporator and CC has much great impacts on the performance of LHP because the tilt of evaporator could change the heat and mass transfer process in evaporator and CC significantly. So far, there has been some literature that reported the effect of evaporator tilt on LHP performance. Ref [20] investigated the operating temperature of a LHP without secondary wick under terrestrial surroundings experimentally. The evaporator tilt was found to have a significant effect on the operating temperature of LHP. The operating temperature was much higher when the evaporator was above the CC, and the weak cooling effect of returning liquid on the vapor in CC or evaporator core was considered as the main reason. Ref [21] investigated the tilt effects on the operation of LHP at small heat load, and the test results showed that the tilt of evaporator affected the operating of LHP by changing the void fraction inside evaporator core. Ref [22] investigated the behaviors of a flat-oval evaporator LHP under different orientations in two perpendicular planes. Ref [23] studied the operating performance of a LHP with liquid guiding holes. The research found that, when the tilt angle between evaporator and CC increased, the change of operating temperature was disparate within different heat load range. Ref [24] tested a miniature loop heat pipe under horizontal and four vertical orientations. The operating temperature under the orientation “evaporator above CC” was quite special. Ref [25] studied the effect of tilts on the operation of a miniature LHP with two evaporators and two condensers. The heat transport capability decreased with an increasing adverse tilt angle.

As briefly reviewed above, NCG and the tilt of evaporator both had great effects on the performance of LHP under terrestrial conditions. On one hand, the existence of

NCG would usually affect the steady state operation of LHP adversely, such as the degradation of heat transfer performance. On the other hand, the evaporator tilts could have favorable or adverse effect on the performance depending on the specific tilt. The effects of the two factors would usually coexist in the practical terrestrial applications of LHP, and the research on their coupling effect was necessary consequently. However, although the effect of NCG and that of evaporator tilt have been studied in depth respectively, few studies have investigated the coupling effect of them, and their coupling effect and corresponding mechanism were still vague. The main objective of this paper is to experimentally investigate the effects of NCG on the performance of LHP under different tilts and the corresponding physical mechanism was analyzed theoretically based on the results of the experiments.

2. Experimental setup

2.1. Experimental apparatus

The schematic of the experimental apparatus is shown in Fig. 1. The experimental apparatus included the tested LHP, DC power supply, coolant circulation device, data acquisition system and air conditioning system. As shown in Fig. 2，the tested LHP in this paper is an ammonia-stainless steel loop heat pipe, consisting of an evaporator, a compensation chamber, a condenser, liquid and vapor lines. The basic parameters of the tested LHP were illustrated in Table 1, where OD/ID represent the outer/inner diameters respectively. The vapor line, liquid line and condenser line were all smooth stainless steel tubes. Fig. 3 showed the photo of evaporator and CC, and Fig. 4 showed the internal structure of the evaporator and the CC. The evaporator and CC were not coaxial, and the evaporator casing was tangent to the CC casing. The primary wick was sintered with nickel powder and the evaporator core was filled with stainless steel wire mesh (not displayed by Fig. 4) as the secondary wick.

The heat load was applied to the evaporator by the kapton heater glued closely on the surface of the evaporator and the different heat loads were simulated by changing the output current of the DC power supply. Because of the contact thermal resistance

between the evaporator casing and the kapton heater, the temperature difference between them would rise with the increase of heat load. Limited by the maximum allowable temperature of the kapton heater (about 120 °C), the maximum heat load was 135 W. As shown in Fig. 5, the condenser line was brazed on the groove of copper plate and the copper plate was glued to the two surfaces of an aluminum cold plate with thermal grease. The cold plate was cooled by a temperature-controlled coolant circulation machine. The pipes connecting cold plate and coolant circulation machine were covered with rubber foam insulation material. The thermal conductivity of the insulation material was 0.034 W/(m·K) and the thickness was about 1 cm. Since the specific heat capacity of coolant (water) was huge and the connecting pipes were insulated, the heat sink temperature was considered equal to the temperature of coolant in coolant circulation machine. The temperature control precision of heat sink was ±0.5 °C.

Eighteen type T thermocouples were attached on the outer surface of the tested LHP to monitor the temperature along the loop and the measure point locations were displayed in Fig. 6. The Data acquisition system consisted of a computer (with Benchlink Data Logger 3 software) and an Agilent 34970A data acquisition module. The measured temperature data was recorded and stored every 5 seconds. The tilt angle of evaporator was adjusted by raising the end of evaporator or CC. The geometric centers of evaporator and condenser were placed at the same level of height in all experiments of this paper and the height difference was less than 2 cm. In order to reduce the heat transfer between the tested LHP and ambient, all components of the tested LHP were covered by rubber foam insulation material. The ambient temperature was controlled through the air conditioning system of which the temperature control accuracy was ±2 °C.

2.2. Experimental conditions

As shown in Fig. 7, the symbol β refers to the angle between the evaporator axis and the horizontal plane, and β is defined as positive when the evaporator is higher

than CC. The condition $\beta>0°$ was called adverse tilt and $\beta<0°$ was favorable tilt. In order to ensure the liquid supply to the wick, the evaporator was placed near the bottom of CC in this experiment. The experimental conditions were illustrated in Table 2. The influences of three typical tilt angles on the temperature in the case with and without NCG were investigated in this paper. Considering the impact of temperature hysteresis phenomenon [26], the heat load cycle experiments were carried out for every experimental condition in Table 2. The variation of heat load was introduced in

Table 3. The heat sink temperature and ambient temperature were controlled at 20 °C and 18 °C respectively throughout the experiment.

2.3. Experimental procedure

In order to minimize the interference of NCG adsorbed on the inner surface, the clean of LHP before charge is necessary. Specific cleaning procedure were introduced detailedly in Ref [16], and a brief summary was made below: (1) vacuumize the internal space of the tested LHP and charge 11 g ammonia into the loop; (2) operate the LHP for about one hour; (3) repeat the above procedure for three times and the cleaning procedure was finished after the fourth charge.

After the clean and charge procedure was completed, the tilt angle of evaporator and the ambient temperature were adjusted to the designed values firstly and the tested LHP would be left for more than 2 hours to reduce the impact of initial state. Before the preset heat load was applied to the evaporator, the heat sink temperature had been controlled at the designed temperature for over 30 minutes. In the experiment process, the judgment standard of steady state operation was as follow: within 30 minutes, the temperature change was less than 1.0 °C or the temperature fluctuated periodically[16]. After the completion of experiments without NCG, the LHP was cooled to ambient temperature and nitrogen was injected into the LHP with NCG injection system. After injection, the experiments with NCG could be conducted as planned.

Fig. 8 was the schematic of NCG injection system and the charging method of NCG can be described as below. (1) only valve 1 was opened to evacuate the container and related pipelines; (2) only valve 2 was opened to inject nitrogen into the container until it reached the required pressure; (3) only valve 3 was opened to charge nitrogen into LHP utilizing the pressure difference. More detailed charging procedure of NCG was introduced in Ref. [16] and the maximum uncertainty of the NCG inventory in this paper was about ±3%.

2.4. Data processing and uncertainty analysis

In this experiment, the heat load applied to the evaporator could be calculated by Eq. (1). The current through the heater could be measured by the DC power supply and the measurement uncertainty was 0.1%. The nominal resistance of kapton heater was 20.5 Ω. Considering the impact of temperature, the actual resistance of the heater was experimentally verified over the allowable temperature range and the maximum uncertainty was 0.81%. As a result, the maximum uncertainty of heat load was 0.83%.

$$Q = I^2 R_{heater} \tag{1}$$

The temperature used for analysis below was the average temperature results in forward motion (step increase of heat load) and backward motion (step decrease of heat load) of heat load cycle. Considering the effects of thermocouple stability, junction end and data logger, the thermocouples were calibrated with the help of two standard platinum resistance temperature sensors in the temperature range from 20 to 60 °C and the maximum measurement error of temperature was ±0.46 °C.

The thermal resistance of the condenser could be calculated by Eq. (2)

$$R_{cond} = \frac{T_{CC} - T_{sink}}{Q} \tag{2}$$

and the maximum uncertainty of condenser thermal resistance was about 7.0%.

3. Results and discussions

Fig. 9 and Fig. 10 displayed the temperature characteristics under different evaporator tilts in the case without and with NCG respectively. Note that when the NCG inventory was 8×10^{-5} mol, the temperature of kapton heater would exceed the allowable temperature at all experimental conditions and the LHP must be shut down for safety. Obviously, whether or not there was NCG in LHP, the temperature was the highest in the case β=15° and the lowest in the case β=-15° when heat load was the same. However, the changes of temperature caused by favorable tilt (β=-15°) or adverse tilt (β=15°) were affected by the injection of NCG. The reasons for the changes would be analyzed and discussed in detail later.

3.1 Horizontal attitude (β=0°)

Fig. 11 illustrated the temperature characteristics in the case with and without NCG when β=0°. In the case without NCG, the evaporator outlet temperature remain the same approximately and the CC temperature decreased with the increase of heat load within the whole heat load range. After the injection of NCG, both evaporator outlet temperature and CC temperature were significantly higher than that in the case without NCG. In addition, the increment of temperature caused by the injection of NCG ΔT_{NCG} declined with the increase of heat load. More precisely, ΔT_{eva_out} was 8.4 °C when the heat load was 15 W and only 3.7 °C when the heat load was 135 W; ΔT_{CC} was 8.9 °C when the heat load was 15 W and only 1.2 °C when the heat load was 135 W. Fig. 12 displayed the heat load dependence of the condenser thermal resistance. The injection of NCG increased the condenser thermal resistance and the effect decreased with the increase of heat load.

Previous researches had shown that the energy balance of the working fluid in evaporator core and CC determined the temperature of LHP. According to Eq. (3), the CC temperature was decided by the heat leak from evaporator to CC Q_{leak} when test conditions were the same.

$$T_{\mathrm{CC}} = \frac{Q_{leak}}{\dot{m}C_p} + T_{return} \tag{3}$$

As shown by Eq. (4), Q_{leak} consisted of two parts in general: the heat leak caused by heat conduction and heat convection Q_1 and the heat leak caused by the boiling in evaporator core Q_2. According to the research in Ref [16], the majority of NCG accumulated in CC in the process of operation and produced partial pressure P_{NCG}, Q_1 was the function of P_{NCG} and increased when P_{NCG} increased. In addition, a small amount of NCG adsorbed on the inner surface of LHP or dissolved in the liquid working fluid, which could increase nucleation sites and facilitate the nucleate boiling in evaporator core. Usually, there was large uncertainty about nucleate boiling, hence Q_2 was very hard to define by a simple equation. Therefore, the presence of NCG

would increase Q_{leak} and further increased the CC temperature.

$$Q_{leak} = Q_1 + Q_2 = G_{eva,\mathrm{CC}}\left(T_{eva} - T_{\mathrm{CC}}\right) + Q_2 = G_{eva,\mathrm{CC}}\frac{\partial T}{\partial P}\left(P_{\mathrm{NCG}} + \Delta P_{loss}\right) + Q_2 \qquad (4)$$

In general, the impact of NCG on Q_1 and Q_2 was quite different. NCG increased Q_1 by generating partial pressure P_{NCG} and even a small amount of NCG could cause a significant increase of Q_1. As heat load increased, more working fluid flowed into CC and the volume of gas in evaporator core and CC declined, so the partial pressure of NCG went up. Consequently, the heat leak increase caused by NCG $\Delta Q_{1,\mathrm{NCG}}$ would rise with the increase of heat load. However, the promotion effect of NCG on nucleate boiling was usually not obvious, so the influence of NCG on Q_2 was relatively small. In summary, the heat leak increase caused by the presence of NCG $\Delta Q_{leak,\mathrm{NCG}}$ would increase with the increase of heat load.

When the tilt angle β=0°, the gas and liquid distribution in the evaporator and CC was illustrated by Fig. 13. Because the CC and the evaporator were non-concentric, and there was a secondary wick installed in the evaporator core and CC, the evaporator core was fully filled with liquid in the experiments under horizontal attitudes. As shown in Fig. 13, the bubbles would generate on the inner surface of wick and flow to CC. The returning subcooled liquid would flow to CC along the evaporator core after exiting the bayonet and be heated by the radial heat leak in this process. As a result, more bubbles would generate in the part near the CC. As the heat load increased, the heat leak increase caused by NCG $\Delta Q_{leak,\mathrm{NCG}}$ became larger. At the same time, the augmented heat load also increased the mass flow rate and cooling capability of returning subcooled liquid. As a result, the returning subcooled liquid would have a better disturbance effect on the liquid in evaporator core and provide bigger cooling capability. Because almost the entire evaporator core could be cooled well, as heat load increased, the growth rate of cooling capability exceeded that of $\Delta Q_{leak,\mathrm{NCG}}$. The heat leak was better balanced and the increment of temperature ΔT_{NCG} reduced with the augmentation of heat load.

3.2 Favorable tilt (β=-15°)

Fig. 14 displayed the heat load dependence of evaporator outlet and CC temperature before and after the injection of NCG when β=-15°. In the case without NCG, the temperature of evaporator outlet and CC displayed an approximately U-shaped curve. Compared with the situation β=0°, the temperature at β=-15° was lower. Similarly, the injection of NCG also caused the increase of temperature. The increment of CC temperature caused by NCG ΔT_{CC} decreased approximately with the increase of heat load, which was similar to the case β=0°. However, the reduction of ΔT_{CC} was relatively insignificant compared with the case β=0°. ΔT_{CC} was 1.7 °C when the heat load was 15 W and less than 0.5 °C when the heat load was 135 W. The increment of evaporator outlet temperature caused by NCG ΔT_{eva_out} was almost the same (about 4.6 °C) within the whole heat load range. Fig. 15 was the corresponding heat load dependence of condenser thermal resistance. Compared with horizontal attitude, the change of condenser thermal resistance caused by NCG injection was relatively small when the heat load was not too large.

Fig. 16 illustrated the gas and liquid distribution in evaporator and CC when β was -15°. The tilt of evaporator significantly changed the gas/liquid distribution and further affected the energy balance of the working fluid in evaporator core and CC. Since the temperature was much lower than the liquid in evaporator core and CC, the density of the returning subcooled liquid was larger. After exiting the bayonet, the returning subcooled liquid with larger density would collect at the evaporator core portion away from CC as a result of the influence of gravity and have difficulty flowing to CC. The evaporator core portion away from CC would be cooled effectively and few bubbles would generate here. In addition, the carrying effect of returning liquid abated due to the influence of gravity, and the evaporator core portion near CC was cooled mainly through the thermal conduction of liquid working fluid. The evaporator core portion near CC could not be cooled effectively and more

bubbles would generate here. As a result, the cooling effect of returning subcooled liquid became more uneven and the cooling capacity of the subcooled liquid was wasted. With the increase of heat load, the augmentation of mass flow rate enhanced the heat transfer between returning subcooled liquid and the fluid in evaporator core and CC. However, the main cooling object of the returning subcooled liquid was the evaporator core portion away from CC and the enhancement of cooling effect on the rest part was limited. As a result, the overall cooling effect enhancement of returning subcooled liquid caused by the augmentation of heat load was weaker than the case β=0°. Therefore, with the rise of heat load, the increment of CC temperature caused by NCG ΔT_{CC} did not descend obviously compared with the case β=0°.

3.3 Adverse tilt (β=15°)

Fig. 17 displayed the temperature characteristics in the case β=15°. According to Fig. 17, the minimum evaporator outlet temperature corresponded to a heat load of 90 W in the case without NCG. The CC temperature decreased with the increase of heat load within the whole heat load range. Another noteworthy phenomenon was that the increase of evaporator outlet temperature caused by adverse tilt in this paper was only about 7 °C (as illustrated by Fig. 9), which was much lower than that in Ref [20]. This might be related to the installation of secondary wick in evaporator core and CC.

Expectedly, the temperature also increased after the injection of NCG. The increment of CC temperature ΔT_{CC} changed little with the increase of heat load, which was about 1.6 °C. The evaporator outlet temperature ΔT_{eva_out} increased slightly with the augmentation of heat load correspondingly. Precisely, the temperature increment was 1.1 °C and 4.0 °C when the heat load was 15 W and 135 W respectively. Fig. 18 showed the corresponding heat load dependence of the condenser thermal resistance under adverse tilt. It could be seen that the increment of the condenser thermal resistance caused by NCG changed little with the augmentation of heat load.

When the tilt angle β=15°, as shown in Fig. 19, the gas and liquid distribution in evaporator and CC was quite different from the other two cases. A small area at the bottom of evaporator core could be cooled sufficiently by the returning subcooled liquid because of gravity. However, the rest part of evaporator core almost could not be affected by the influence of the returning subcooled liquid because the thermal conductivity of the gas was much lower than that of the liquid. There was a large area of gas/liquid interface in evaporator core and the liquid evaporated on the interface continuously. Therefore, the increased mass flow rate of returning subcooled liquid could hardly enhance the overall cooling effect and the growth of $\Delta Q_{leak,\mathrm{NCG}}$ could not be balanced effectively. Consequently, ΔT_{CC} changed little and ΔT_{eva_out} went up gradually.

As for the temperature rise caused by NCG in the case β=15° was relatively small, the possible reason was as follows. Because there was little liquid in evaporator core in the case β>0°, the heat leak caused by nucleate boiling Q_2 dominated the total heat leak. However, the promotion effect of NCG on nucleate boiling was usually not obvious enough, so the influence of NCG on heat leak was relatively small and the temperature rise caused by NCG was the smallest in the case β=15° consequently.

According to the analysis above, NCG could lead to an increment on the temperature of LHP under all three different evaporator tilts. However, the heat load dependence of ΔT_{NCG} was different under various tilts, which led to an interesting coupling effect on temperature curves.

4. Conclusions

The steady state characteristics of a LHP with NCG under different evaporator tilts were experimentally investigated in the gravitational field. The main conclusions of this research can be summarized as follows:

- No matter whether there is NCG in the LHP, the temperature under adverse

tilt is higher than that under horizontal attitude and the temperature under favorable tilt is the lowest.

- NCG can cause the temperature of LHP to increase regardless of the tilt angle of evaporator, but the temperature increment caused by NCG in the case β>0° seems to be relatively small.
- The heat load dependence of ΔT_{NCG} was different under various tilts: in the case β=0°, ΔT_{eva_out} changed from 8.4 °C to 3.7 °C when the heat load increased from 15 W to 135 W; in the case β=-15°, ΔT_{eva_out} was about 4.6 °C and changed little within the heat load range; when β=15°, ΔT_{eva_out} is only 1.1 °C-4.0 °C although the temperature was the highest.

Acknowledgments

This work was supported by the National Natural Science Foundation of China (Nos. 51576010 and 51776012) and the Beijing Natural Science Foundation (No. 3182023). The support provided by China Scholarship Council (CSC) during a visit of Xiaobin Shen to the University of Leeds is also acknowledged. The authors are very grateful to Bing Sun, Xueqin Bu and Rui Yang in Beihang University for their help in this paper.

Nomenclature

C_p	specific heat at constant pressure (J/(kg·K))
G	thermal conductance (W/K)
I	current (A)
m	mass (kg)
P	pressure (Pa)
Q	heat (W)
R	electric resistance (Ω), thermal resistance (°C/W)
T	temperature (°C)

Subscripts

eva	evaporator
heater	kapton heater
leak	heat leak
loss	pressure loss of the flow
return	return subcooled liquid
sink	heat sink

References

[1] J. Ku, Operating Characteristics of Loop Heat Pipes, 29 Th Int. Conf. Environ. Syst. (1999) 16. doi:10.4271/1999-01-2007.

[2] Y.F. Maydanik, Loop heat pipes, Appl. Therm. Eng. 25 (2005) 635–657. doi:10.1016/j.applthermaleng.2004.07.010.

[3] K. Nakamura, K. Odagiri, H. Nagano, Study on a loop heat pipe for a long-distance heat transport under anti-gravity condition, Appl. Therm. Eng. 107 (2016) 167–174. doi:10.1016/j.applthermaleng.2016.06.162.

[4] L. Mottet, M. Prat, Numerical simulation of heat and mass transfer in bidispersed capillary structures: Application to the evaporator of a loop heat pipe, Appl. Therm. Eng. 102 (2016) 770–784. doi:10.1016/j.applthermaleng.2016.03.143.

[5] M. Nishikawara, H. Nagano, M. Prat, Numerical study on heat-transfer characteristics of loop heat pipe evaporator using three-dimensional pore network model, Appl. Therm. Eng. (2016). doi:10.1016/j.applthermaleng.2017.02.050.

[6] G. Wang, D. Mishkinis, D. Nikanpour, Capillary heat loop technology: Space applications and recent Canadian activities, Appl. Therm. Eng. 28 (2008) 284–303. doi:10.1016/j.applthermaleng.2006.02.027.

[7] J.I. Rodriguez, A. Na-nakornpanom, In-Flight Performance of the TES Loop Heat Pipe Heat Rejection System – Seven Years In Space, 42nd Int. Conf. Environ. Syst. (2012) 1–10. doi:10.2514/6.2012-3500.

[8] K. Goncharov，O. Golovin，V. Kolesnikov，Zhao Xiaoxiang, Development and flight operation of LHP used for cooling nickel-cadmium batteries in Chinese meteorological satellites FY-1, in: 13th Int. Heat Pipe Conf. vol.1 13th, 2004.

[9] I. Introduction, Performance of COMMx Loop Heat Pipe on TacSat 4 Spacecraft, 42nd Int. Conf. Environ. Syst. (2012) 1–9.

doi:10.2514/6.2012-3498.

[10] M.K. Choi, BAT Loop Heat Pipe #0 Temperature Droop Problem and Solution after Its Primary Heater Controller Failure, 41st Int. Conf. Environ. Syst. (2011) 1–13. doi:doi:10.2514/6.2011-5098.

[11] C. Baker, C. Butler, P. Jester, E. Grob, Geoscience Laser Altimetry System (GLAS) Loop Heat Pipe Anomaly and On Orbit Testing, in: 41st Int. Conf. Environ. Syst., American Institute of Aeronautics and Astronautics, Reston, Virigina, 2011: pp. 1–10. doi:10.2514/6.2011-5209.

[12] W. Larson, J. Wertz, Space Mission Analysis and Design, 2 (1992) 5192.

[13] M.N. Nikitkin, W.B. Bienert, K.A. Goncharov, Non Condensable Gases and Loop Heat Pipe Operation, (1998). doi:10.4271/981584.

[14] K.R. Wrenn, D.A. Wolf, E.J. Kroliczek, Effect on Noncondensible Gas and Evaporator Mass on Loop Heat Pipe Performance, (2000). doi:10.4271/2000-01-2409.

[15] H. ISHIKAWA, T. OGUSHI, T. NOMURA, H. NODA, H. KAWASAKI, T. YABE, Study on Heat Transfer Characteristics of Reservoir Embedded Loop Heat Pipe (2nd Report, Influence of Non Condensable Gas on Heat Transfer Characteristics), Trans. Japan Soc. Mech. Eng. Ser. B. 73 (2007) 847–854. doi:10.1299/kikaib.73.847.

[16] J. He, G. Lin, L. Bai, J. Miao, H. Zhang, Effect of non-condensable gas on the operation of a loop heat pipe, Int. J. Heat Mass Transf. 70 (2014) 449–462.

[17] P. Prado-Montes, D. Mishkinis, A. Kulakov, A. Torres, I. Pérez-Grande, Effects of non condensable gas in an ammonia loop heat pipe operating up to 125 C, Appl. Therm. Eng. 66 (2014) 474–484. doi:10.1016/j.applthermaleng.2014.02.017.

[18] R. Yang, G. Lin, J. He, L. Bai, J. Miao, Investigation on the effect of thermoelectric cooler on LHP operation with non-condensable gas, Appl.

Therm. Eng. 110 (2017) 1189–1199.
doi:10.1016/j.applthermaleng.2016.09.050.
[19] Y. Zhao, S. Chang, B. Yang, W. Zhang, M. Leng, Experimental study on the thermal performance of loop heat pipe for the aircraft anti-icing system, Int. J. Heat Mass Transf. 111 (2017) 795–803.
doi:10.1016/j.ijheatmasstransfer.2017.04.009.
[20] L. Bai, G. Lin, H. Zhang, D. Wen, Effect of evaporator tilt on the operating temperature of a loop heat pipe without a secondary wick, Int. J. Heat Mass Transf. 77 (2014) 600–603.
doi:10.1016/j.ijheatmasstransfer.2014.05.044.
[21] P. Rogers, Investigation of Low Power Operation in a Loop Heat Pipe, SAE Tech. Pap. (2001) 12. doi:10.4271/2001-01-2192.
[22] S. Becker, S. Vershinin, V. Sartre, E. Laurien, J. Bonjour, Y.F. Maydanik, Steady state operation of a copper-water LHP with a flat-oval evaporator, Appl. Therm. Eng. 31 (2011) 686–695.
doi:10.1016/j.applthermaleng.2010.02.005.
[23] Y. Zhao, S. Chang, W. Zhang, B. Yang, Experimental research on thermal characteristics of loop heat pipe with liquid guiding holes, Appl. Therm. Eng. 101 (2016) 231–238. doi:10.1016/j.applthermaleng.2016.02.106.
[24] Y. Chen, M. Groll, R. Mertz, Y.F. Maydanik, S.V. Vershinin, Steady-state and transient performance of a miniature loop heat pipe, Int. J. Therm. Sci. 45 (2006) 1084–1090. doi:10.1016/j.ijthermalsci.2006.02.003.
[25] H. Nagano, J. Ku, Gravity effect on capillary limit in a miniature loop heat pipe with multiple evaporators and multiple condensers, AIP Conf. Proc. 880 (2007) 3–10. doi:10.1063/1.2437434.
[26] S. V. Vershinin, Y.F. Maydanik, Hysteresis phenomena in loop heat pipes, Appl. Therm. Eng. 27 (2007) 962–968.
doi:10.1016/j.applthermaleng.2006.08.016.

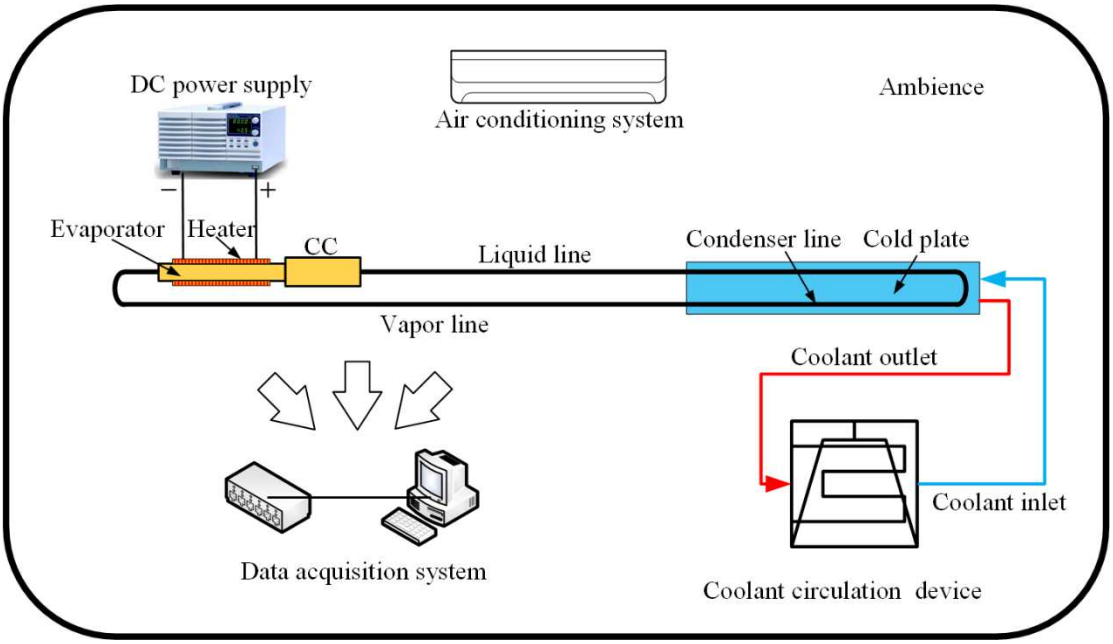

Fig. 1 Schematic of the experimental apparatus

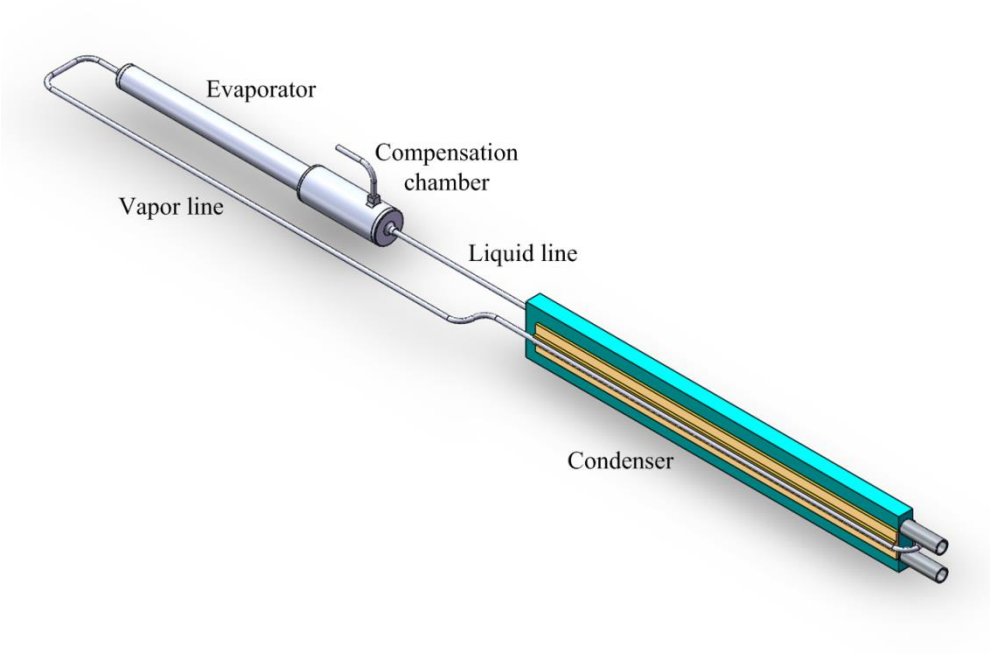

Fig. 2. Schematic of the tested LHP

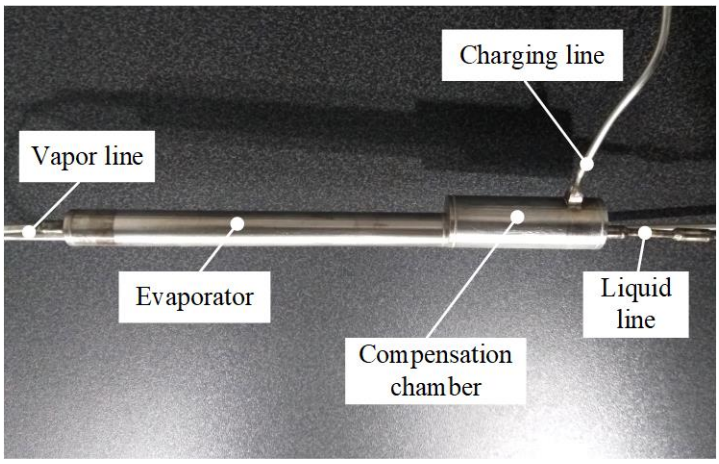

Fig. 3 Photo of the evaporator and CC

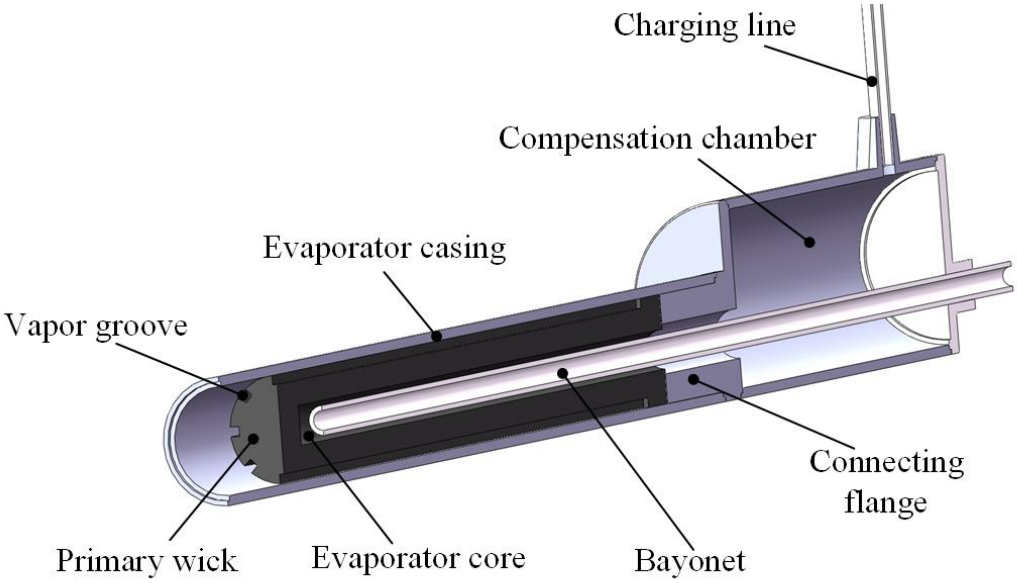

Fig. 4. The internal structure of the evaporator and CC

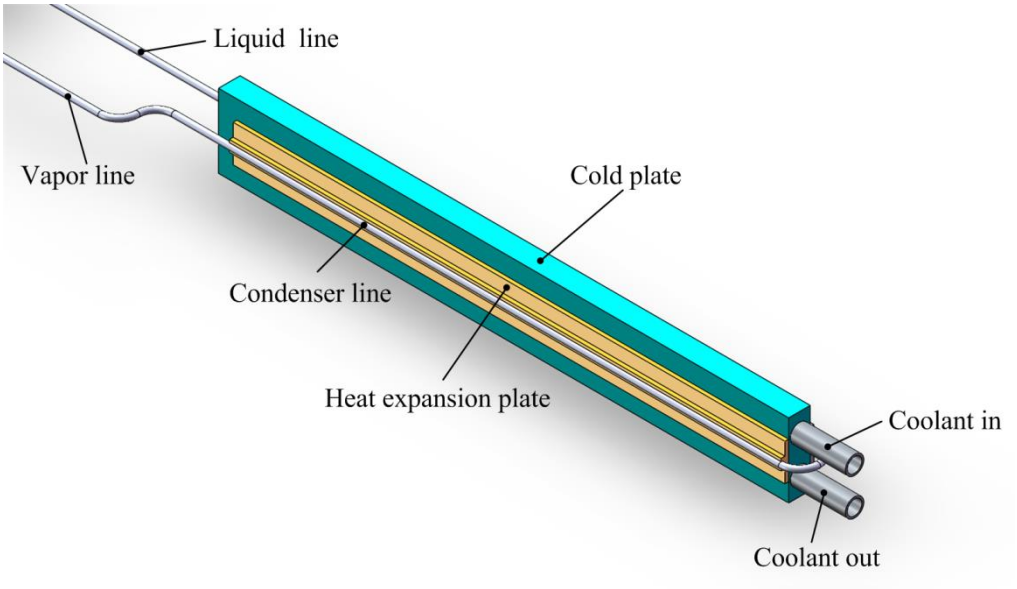

Fig. 5. Schematic of the condenser and cold plate

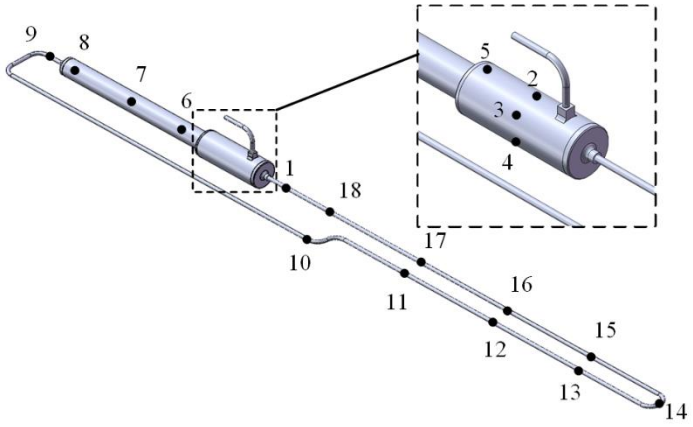

Fig. 6. Thermocouple locations along the loop

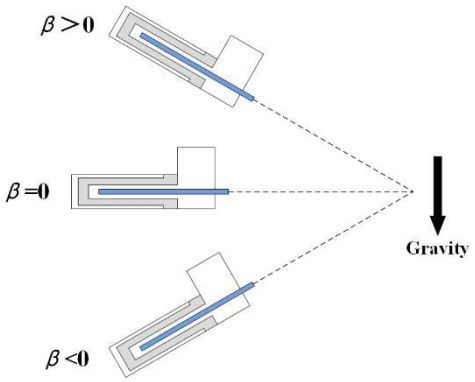

Fig. 7 Schematic of the tilt angle of the evaporator

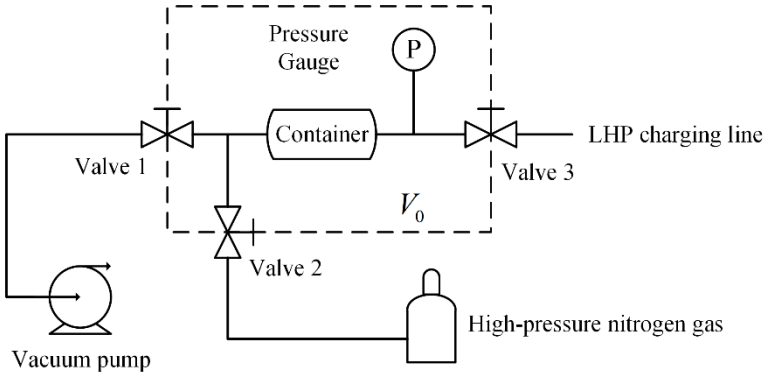

Fig. 8 Schematic of NCG injection system

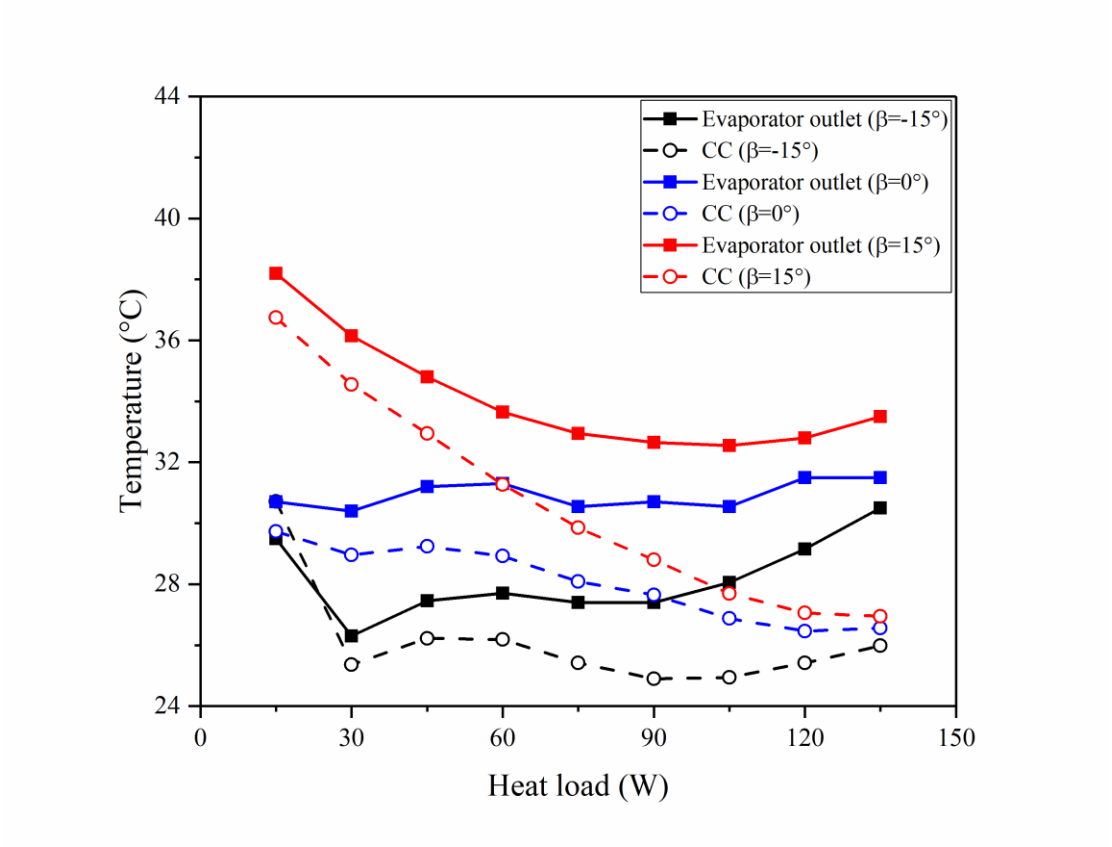

Fig. 9 Temperature characteristics under different evaporator tilts (without NCG)

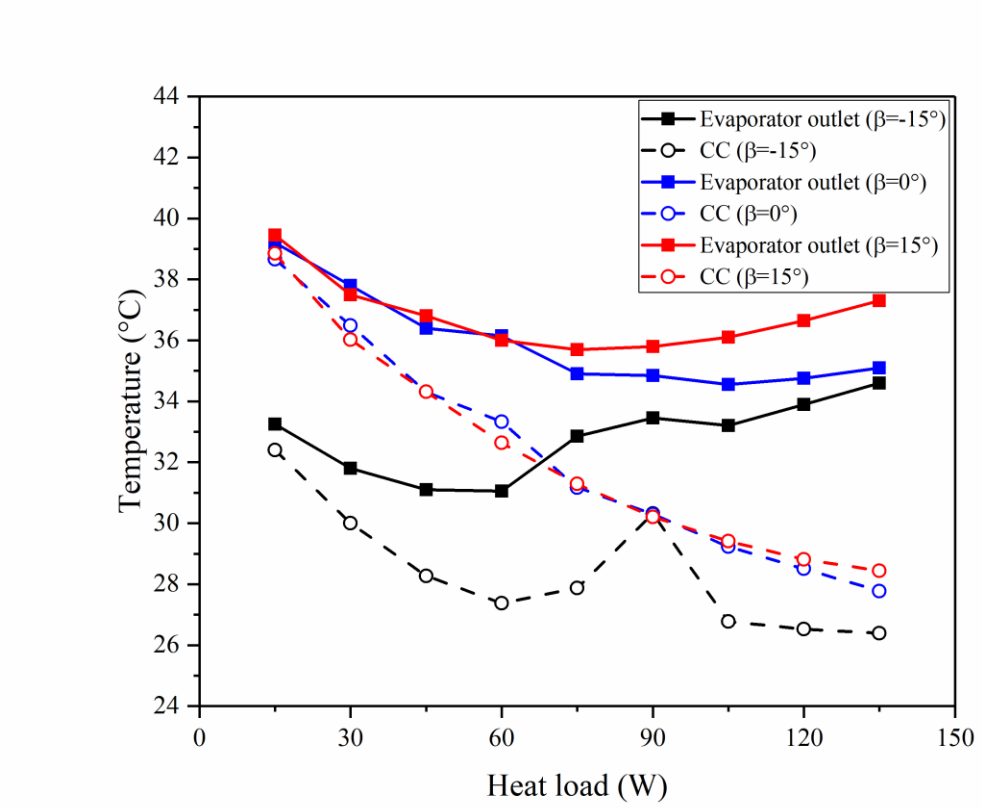

Fig. 10 Temperature characteristics under different evaporator tilts (with NCG)

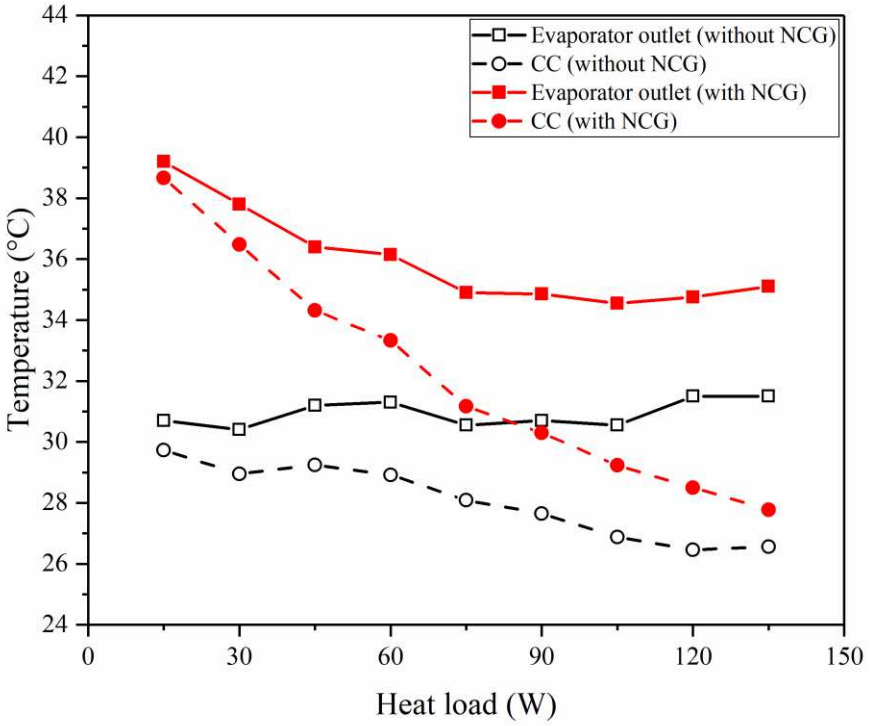

Fig. 11. Temperature characteristics under horizontal attitude (β=0°)

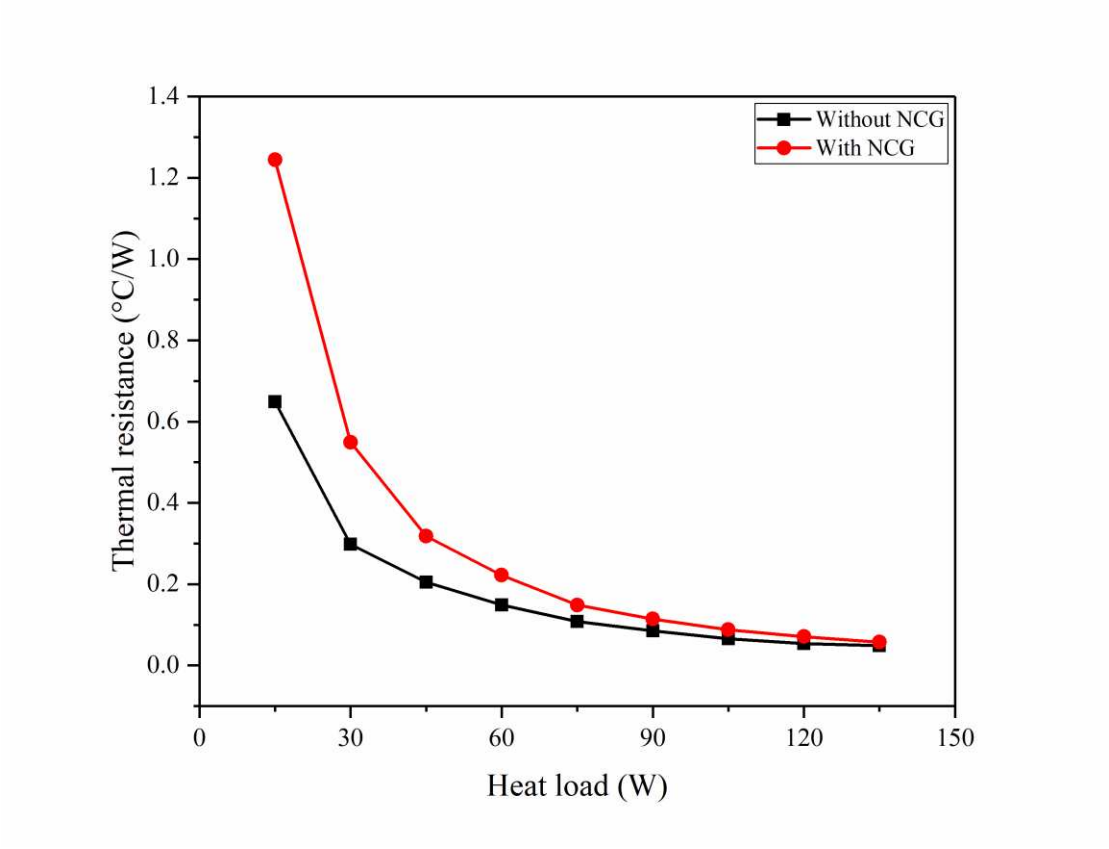

Fig. 12 Heat load dependence of condenser thermal resistance under horizontal attitude (β=0°)

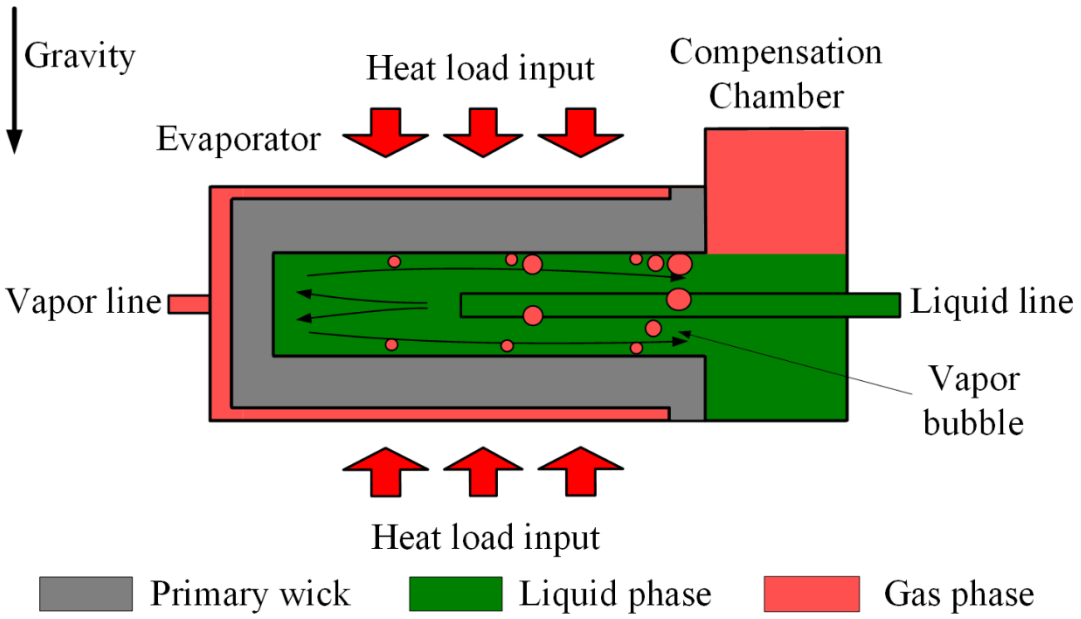

Fig. 13 Gas and liquid distribution in the evaporator and CC under horizontal attitude (β=0°)

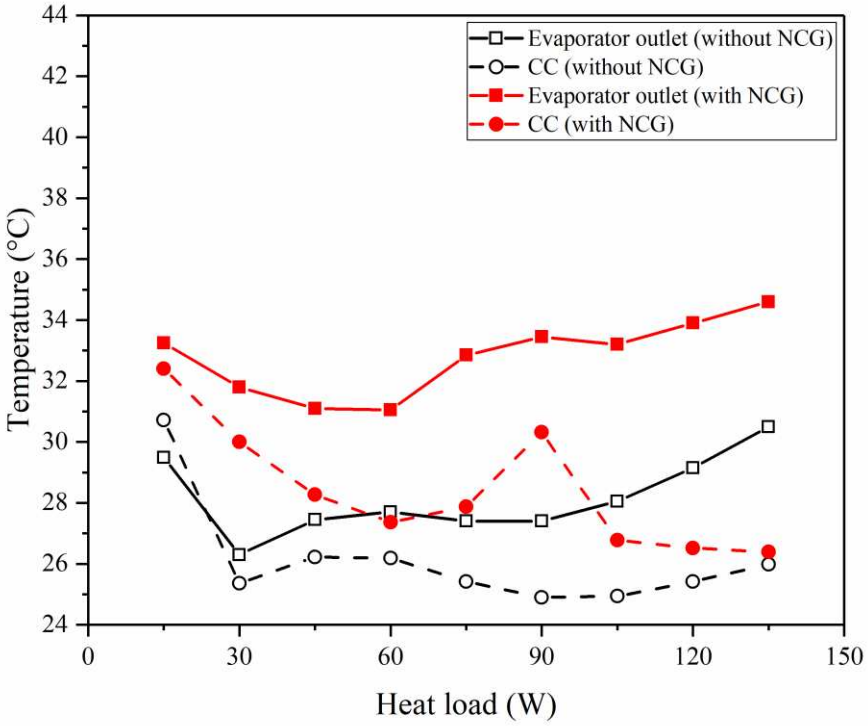

Fig. 14. Temperature characteristics under favorable tilt (β=-15°)

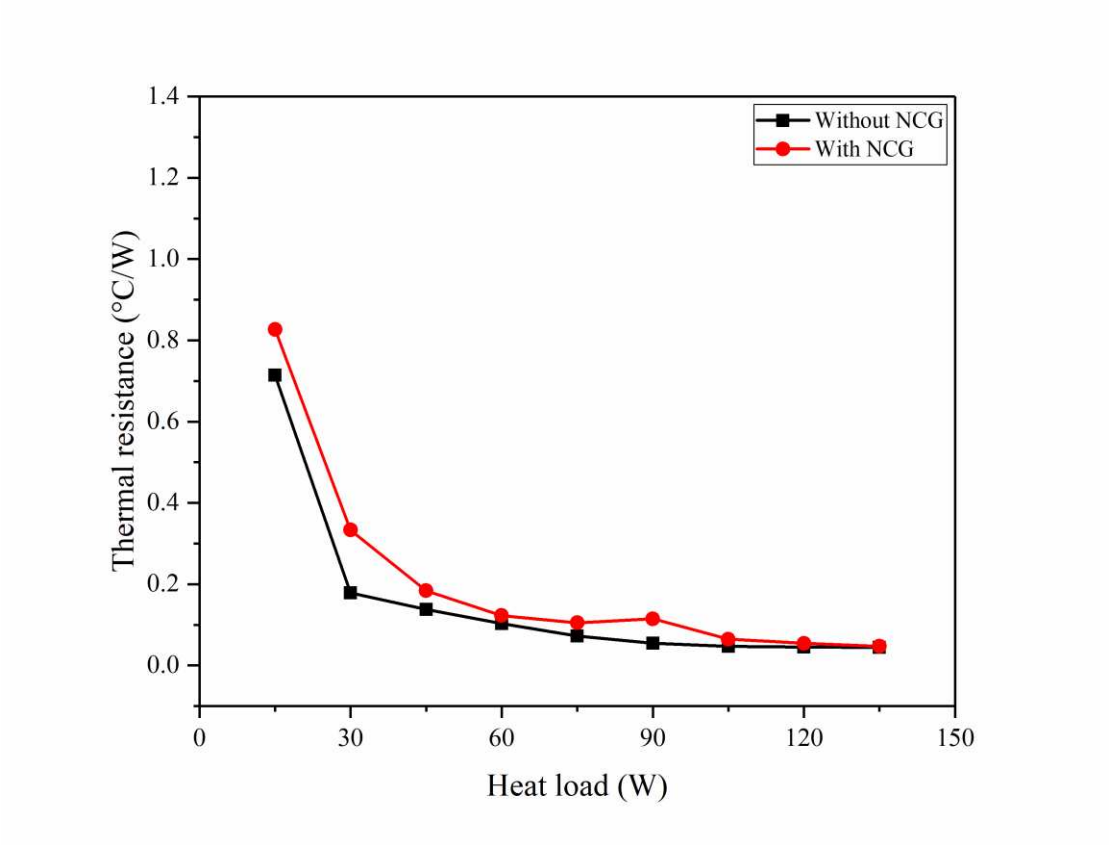

Fig. 15 Heat load dependence of condenser thermal resistance under favorable tilt (β=-15°)

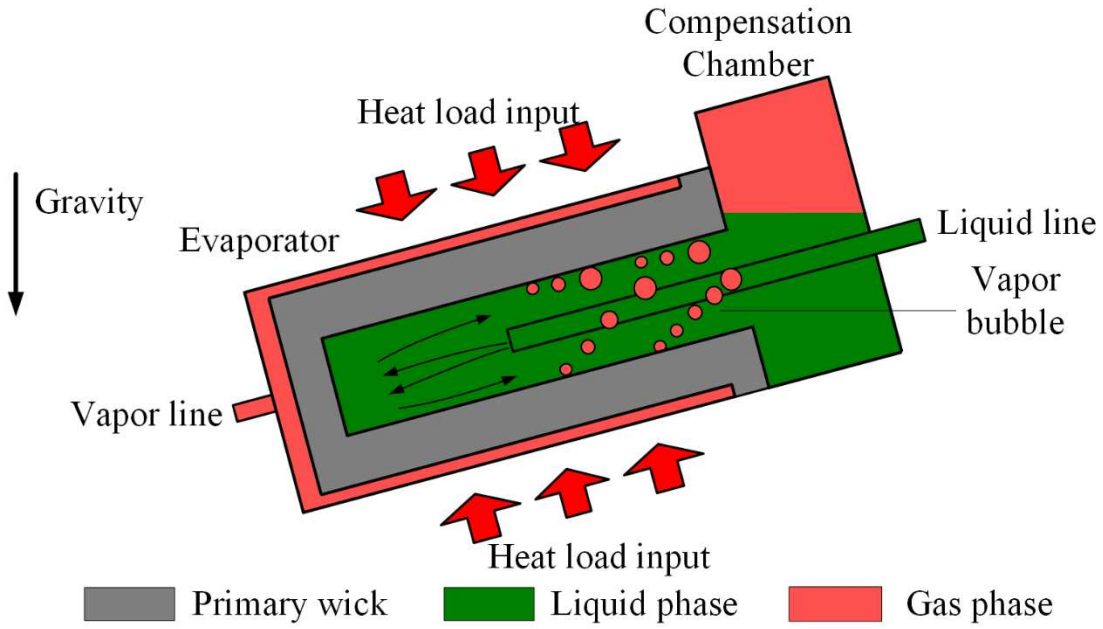

Fig. 16 Gas and liquid distribution in the evaporator and CC under favorable tilt (β=-15°)

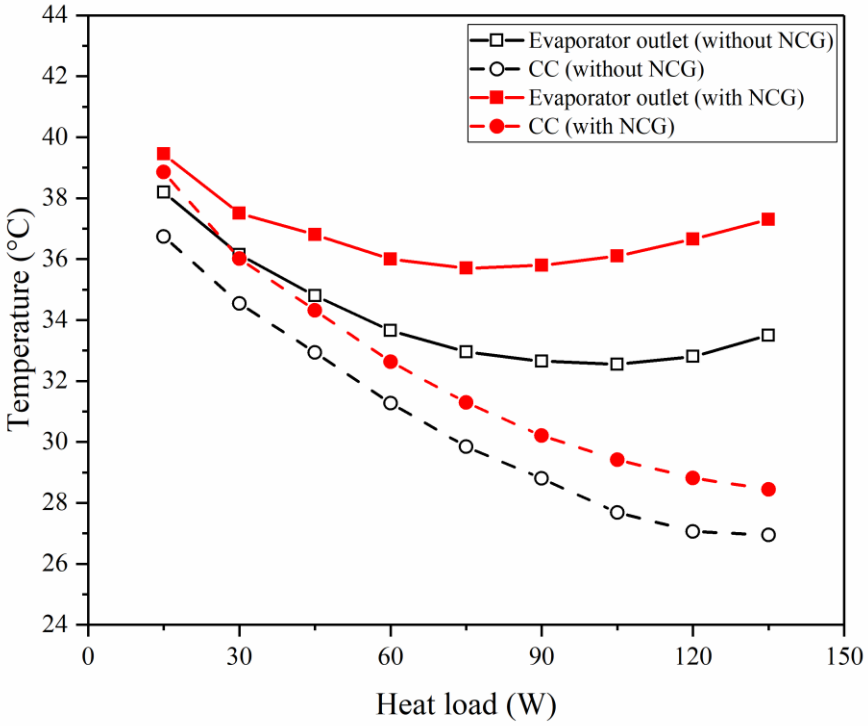

Fig. 17. Temperature characteristics under adverse tilt (β=15°)

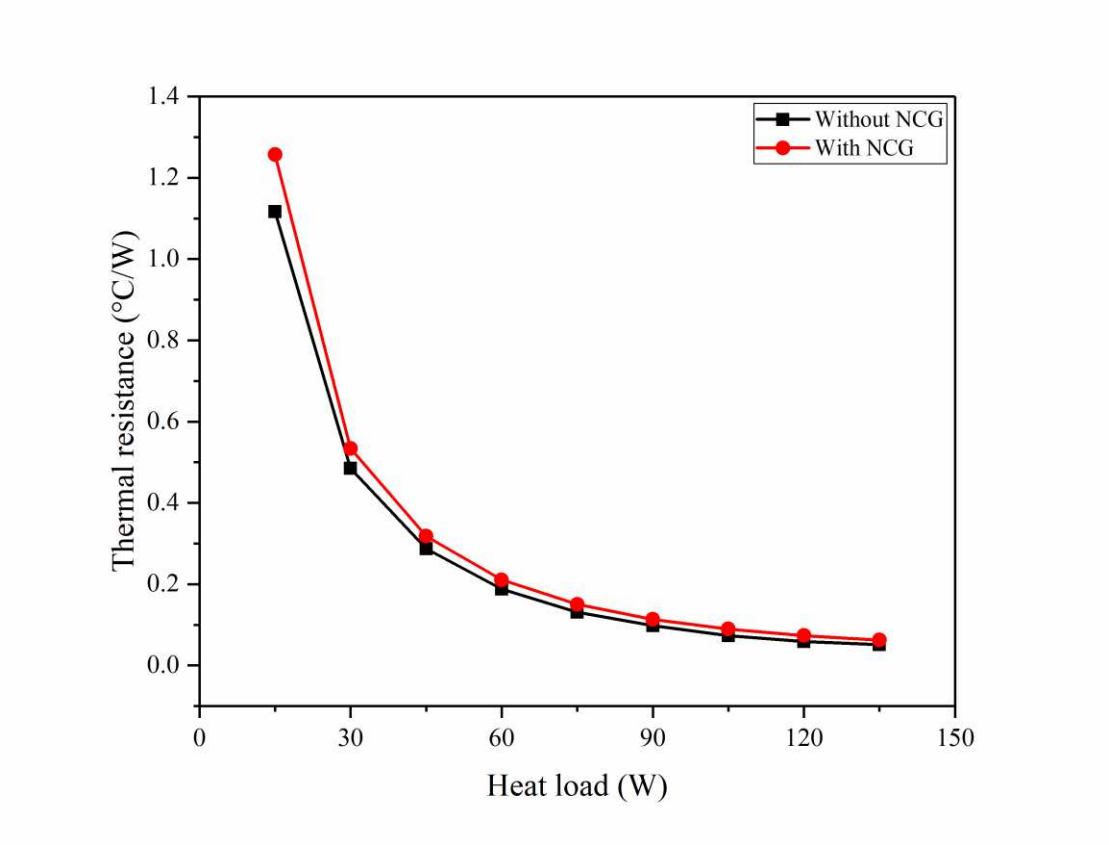

Fig. 18 Heat load dependence of condenser thermal resistance under adverse tilt (β=15°)

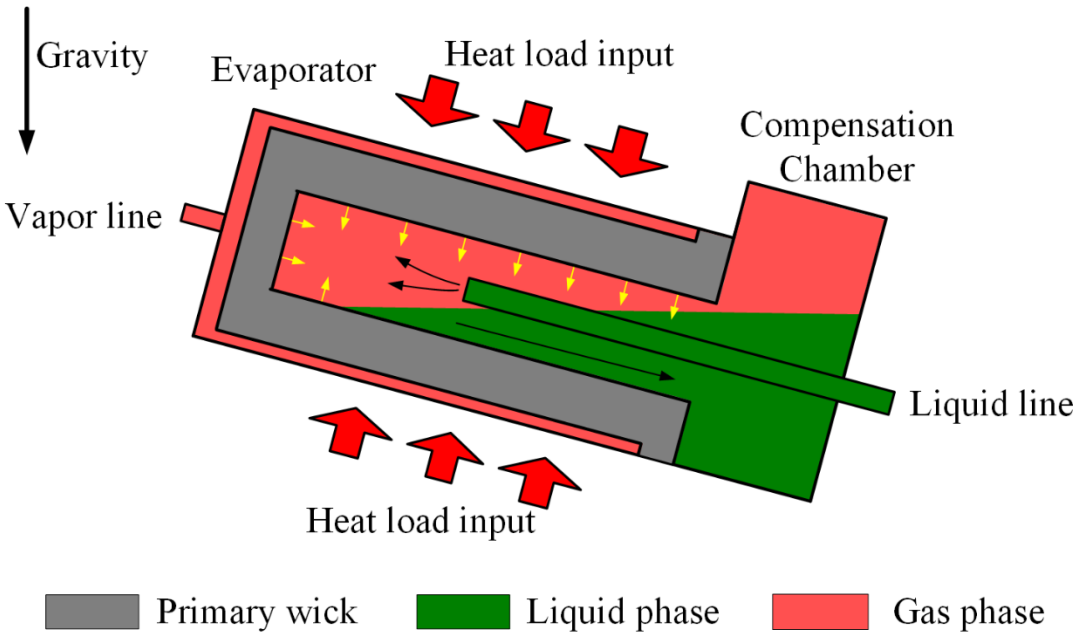

Fig. 19 Gas and liquid distribution in the evaporator and CC (β=15°)

Table 1 Basic parameters of the tested LHP.

Component	Variable	Parameter
Evaporator casing	Material	Stainless steel
	OD/ID×length/mm	13/11×130
Primary wick	Material	Nickel
	OD/ID×length/mm	11/4×100
	Porosity	55.0%
	Maximum pore radius/μm	1.0
Secondary wick	Material	Stainless steel
	Average pore radius/μm	20
Vapor grooves	Number×height×width/mm	8×1×1
Vapor line	Material	Stainless steel
	OD/ID×length/mm	3/2×1160
Condenser line	Material	Stainless steel
	OD/ID×length/mm	3/2×1200
Liquid line	Material	Stainless steel
	OD/ID×length/mm	3/2×900
CC (including the connecting flange)	Material	Stainless steel
	Volume/ml	15.26
Working fluid	Substance	Ammonia
	Fluid inventory/g	11.0±0.1

Table 2 Experimental conditions setup

NCG inventory/$\times 10^{-5}$ mol	Tilt angle of evaporator β/°
0	-15
	0
	15
2	-15
	0
	15
8	-15
	0
	15

Table 3 Heat load variation in the experiments

Heat load interval/W	Variation of heat load/W
15	15-30-45-60-75-90-105-120-135-120-105-90-75-60-45-30-15